

# Fibers Caught in the Knuckles of the Forming Wires: Experimental Measurements and Physical Origins of the Force of Peeling in the Hydroentanglement Process

Ping Xiang<sup>1</sup>, Andrey V. Kuznetsov, Ph.D.<sup>1</sup>, Abdelfattah Mohamed Seyam, Ph.D.<sup>2</sup>

<sup>1</sup>Department of Mechanical and Aerospace Engineering, College of Engineering, North Carolina State University, Raleigh, North Carolina USA

<sup>2</sup>College of Textiles, North Carolina State University, Raleigh, North Carolina USA

Corresponding Author:

Abdelfattah Mohamed Seyam, Ph.D. email: [aseyam@tx.ncsu.edu](mailto:aseyam@tx.ncsu.edu)

## ABSTRACT

In hydroentanglement process, very fine water jets with high pressure impinge on the fiberweb, which is supported by forming wires. The impact of the jets causes fiber entanglement in the fiberweb and produces an integrated fabric with desired performance, texture, and appearance similar to the forming wires. It is important that at the end of the process, the fiberweb can be easily separated from the forming wires. In this paper, the force of peeling required for the separation of the wet, hydroentangled fabric from the forming wires is measured experimentally. A set of experimental trials was conducted to investigate the effects of the jet pressure, fiberweb basis weight, and forming wires mesh size on the peeling force. Visualizing fibers caught in the knuckles of the forming wires under magnification reveals physical mechanisms leading to the formation of the peeling force.

## INTRODUCTION

Hydroentanglement is a mechanical bonding process designed to produce nonwoven fabrics with the texture and appearance that resemble woven and knitted fabrics. In a typical hydroentanglement process, a row or multiple rows of highly pressurized, fine, closely spaced water jets impinge on a fiberweb, which is supported by forming wires (*Figure 1*). Due to the impact of water jets, fibers are displaced and rotated around other fibers that surround them, resulting in fibers twisting and entangling around the neighboring fibers. The fabric produced is held together by the fiber-to-fiber friction. For fibers located in the lower portion of the fiberweb close to the forming wires, it is quite usual to be pushed into the knuckles (the cross-over areas of MD and CD wires, see *Figure 5b*) of the forming

belt. This creates difficulty in separating the fabric from the forming wires. If the required peeling force is large, the structure and properties of the fabric may be compromised during fabric separation from the forming wires (see *Figure 2*). In *Figure 2*, the horizontal direction is the machine direction, and the fabric is separated from the forming belt from the right to the left in the MD (see the horizontal jet streaks on the fabric). The fabric in *Figure 2* is strongly distorted at the edge, and there is even a hole at the fabric edge, which resulted from fabric separation from the forming belt. Thus, if too many fibers are caught in the knuckles of the forming wires, the integrity of the fabric structure is negatively affected. Additionally, the process efficiency is drastically reduced as a result of stops to clean the belt from fibers. If the fibers caught by the forming wires are accumulated and not removed, the performance and texture of the resultant hydroentangled fabric suffer to a great extent.

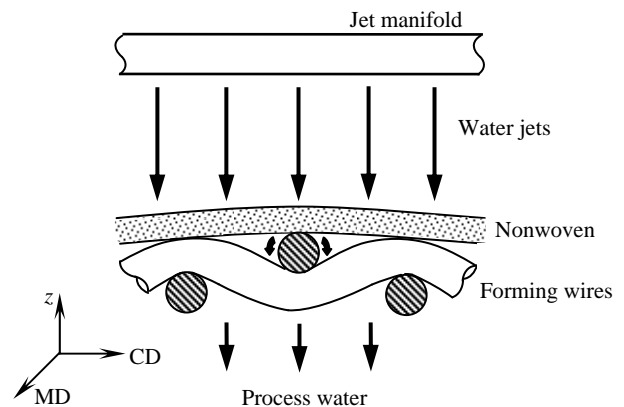


FIGURE 1: Typical cross-section of a hydroentanglement unit



FIGURE 2. Fabric damage as a result of separating the fabric from the forming belt

A considerable amount of research was conducted on technology for hydroentanglement products and process parameters. The effect of the nozzle geometry on the water jet breakup and impact force in the hydroentanglement process was investigated experimentally and numerically in [1,2]. The cavitation and hydraulic flip inside hydroentanglement nozzles were also studied in [3,4]. Effects of the initial fiberweb geometry and pressure distribution between different manifolds of water jets on the properties of hydroentangled fabric were studied experimentally in [5]. The experimental investigation of the effect of fiberweb and fiber properties on the critical water jet pressure and energy consumption was presented in [6].

The fiber orientation and length distribution in hydroentangled fabrics were evaluated in [7] by analyzing two-dimensional SEM images. The relationships between the microstructural variables and fabric mechanical properties (strength and modulus), which were used to estimate the degree of entanglement in hydroentangled fabrics, were also analyzed. The structure-process-property relationships in hydroentangled nonwovens were developed through experimental studies reported in [8].

Research and development work was also focused on reducing the energy consumption in this process. Improving the injector, developing an efficient high pressure pumping system, better fiber composition and web forming method, as well as designing improved piping and vacuum systems were all used to reduce energy consumption [9]. The development of texture during hydroentanglement was examined in [10] as a function of hydroentangling energy. Research reported in [11] showed that

hydroentanglement can be combined with other bonding processes, such as chemical, thermal or hydrogen, to improve fabric properties and reduce the amount of hydroentangling energy required.

Communication with industry experts revealed that fiber entrapment around the forming wires and in the knuckles (and hence the peeling force) poses serious problems, as discussed above. Despite the significant effect of the peeling force on the final fabric properties, no systematic experimental research addressing the peeling force required to separate the fabric from the forming wires in the hydroentanglement process has been reported so far. The authors' previous work [12] was focused on the development of a model for the peeling force. The aim of this paper is to provide a fundamental understanding of the cause of peeling force through systematic experimental investigation of the effects of the process and web parameters (such as the jet pressure, fiberweb basis weight, and forming wires mesh size) and visualizing fibers left caught in the knuckles of the forming wires under magnification.

## EXPERIMENTAL PROCEDURE

### Sample processing and experimental design

To test the peeling force, samples of hydroentangled fabric were produced using Fleissner's hydroentanglement machine available at the facilities of NCRC at NCSU. Four woven forming belts (see *Table I*) were used in the hydroentanglement process, which were provided by the Albany International. The fiberweb and forming belt were moving at a controlled constant speed of 30 m/min.

The highly pressurized water jets impinging on the fiberweb have a diameter of 0.127 mm, and a density of 15.8 jets/cm (40 jets/ inch). Two different carded and crosslapped webs with different basis weights (50 g/m<sup>2</sup> and 100 g/m<sup>2</sup>) were used. The polyester fiber used to form the webs is of linear density 0.168 g/km (1.68 dtex) and of fiber length 38 mm.

A total of 24 hydroentangled fabrics were produced (two basis weights x three pressure levels x four belts). The belts' specifications, pressure levels, and pressure distribution for each manifold are shown in *Tables I* and *II*. Each trial (for the same fabric) was repeated three times to produce total of six samples (two from each trial) five of which were used to measure the peeling force (and one was kept in reserve).

TABLE I. Geometrical parameters of the forming wires

Forming wires	Count (/cm) [/inch]	MD wire diameter (mm)	CD wire diameter (mm)	Open area (%)	Wire cross-section shape	Thickness (mm)
100 mesh	40.0 × 35.4 [100 × 90]	0.11	0.14	29	Round	1.6510
75 mesh	30.0 × 24.4 [75 × 62]	0.15	0.22	26	Round	0.6858
36 mesh	14.2 × 10.6 [36 × 27]	0.40	0.40	25	Round	0.3586
10 mesh	4.3 × 4.3 [11 × 11]	0.89	1.00	35	Round	0.2794

TABLE II. Pressure distribution of different manifolds

Pressure (MPa)		
Manifold No. 1	Manifold No. 2	Manifold No. 3
4	9	9
4	14	14
4	20	20

**Peeling force testing procedure**

After the hydroentanglement process, the wet fabric samples have not been separated immediately from the forming belt. For each fabric/forming wires combination tested, five rectangular samples of the fabric attached to the forming wires of a size of 25 mm × 150 mm (CD × MD) have been cut after each trial.

The separation of the fabric from the forming belt is performed in the machine direction since this is how

it happens in real production. The peeling force was measured using a Sintech tensile tester shown in *Figure 3*. The gauge length between the two jaws initially (before the peeling process) is 75 mm, and the clamping grip pressure used is 10.34 MPa (1500 psi). Before testing the peeling force, the fabric has been partly separated from the forming wires for the length of about 50 mm; then the separated fabric was held in place in the upper jaw of the tensile tester, and the separated forming wire was held in place in the lower jaw (as shown in *Figure 3*). Once the peeling process was started, the upper jaw was moved upward with a constant speed of 0.3 m/min.

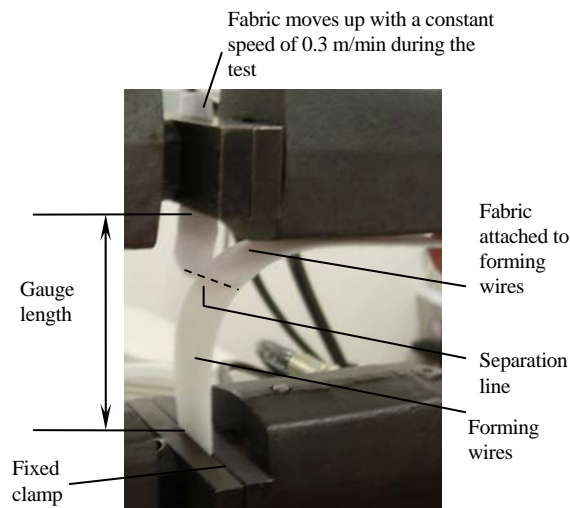


FIGURE 3. Initial state of the fabric partly separated from the forming wires before testing in the Sintech tester

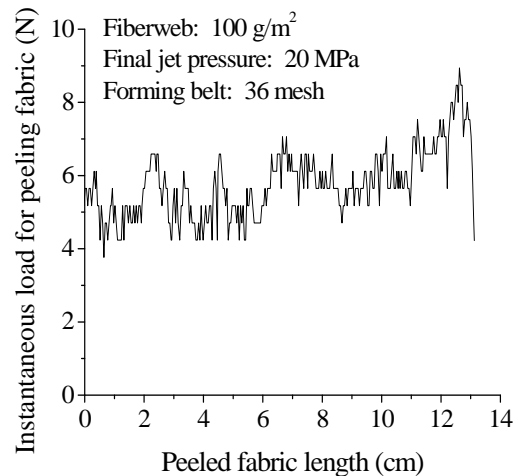


FIGURE 4. A typical graph obtained from the tensile tester

Figure 4 shows a typical graph obtained from the tensile tester. The graph shows only the portion of the distance-force relation after removal of the slackness of the sample. The peaks of the graph represent the instantaneous peeling force, and the average of these peaks is calculated to obtain the peeling force for a given sample. The peeling force of each fabric from a forming belt is calculated by averaging the peeling forces for five samples of the fabric.

## RESULTS AND DISCUSSION

### Peeling force results

The measured peeling forces for each fabric on different forming belts are summarized in Tables III through VI. These tables give the average value of the peeling force and the standard deviation. For most cases the standard deviation does not exceed 10% of the average value. The variation of the peeling force between the measurements is mostly due to the inhomogeneous structure of the fabric/forming belt interface. The peeling force is due to the fibers that are caught in the knuckles of the forming wires; the instantaneous peeling force varies as the separation proceeds from one knuckle to the

next; this is supported by the instantaneous peeling force data shown in Figure 4.

Photographs of the magnified structure of the forming belts after the belt was separated from the fabric are also taken to better understand physical phenomena that induce the peeling force. Figures 5 through 8 show magnified images taken for different webs and different forming belts at jet pressure of 20 MPa. Different magnification is used for different forming belts in order to clearly show the geometry of the forming wires as well as the fibers left caught in the knuckles (the magnifications on the same forming belts are the same for 50 g/m<sup>2</sup> and 100 g/m<sup>2</sup> webs, the exact magnifications are listed in the caption of the corresponding figure).

Figures 5 through 8 show that some fibers are left caught by the forming wires after the fabric is separated from the forming belt. It is evident that for the coarsest 10 mesh forming belt (Figures 5a and 5b), there are more fibers entangled around the forming wires and left caught in the knuckles than for the other forming belts. As the forming belt gets finer, there are fewer fibers left caught by the forming wires. This is especially true for the 100 mesh forming belt

TABLE III. Experimental peeling force data for 10 mesh forming belt

	Fabric processed with 50 g/m <sup>2</sup> web			Fabric processed with 100 g/m <sup>2</sup> web		
	9	14	20	9	14	20
Final jet pressure (MPa)	9	14	20	9	14	20
Peeling force (N/cm)	2.800	3.675	3.850	2.625	2.945	3.325
Standard deviation (N/cm)	0.175	0.225	0.280	0.350	0.263	0.175

TABLE IV. Experimental peeling force data for 36 mesh forming belt

	Fabric processed with 50 g/m <sup>2</sup> web			Fabric processed with 100 g/m <sup>2</sup> web		
	9	14	20	9	14	20
Final jet pressure (MPa)	9	14	20	9	14	20
Peeling force (N/cm)	2.450	3.150	3.325	2.275	2.675	2.975
Standard deviation (N/cm)	0.225	0.085	0.350	0.140	0.175	0.263

TABLE V. Experimental peeling force data for 75 mesh forming belt

	Fabric processed with 50 g/m <sup>2</sup> web			Fabric processed with 100 g/m <sup>2</sup> web		
	9	14	20	9	14	20
Final jet pressure (MPa)	9	14	20	9	14	20
Peeling force (N/cm)	2.100	2.625	2.800	1.925	2.275	2.450
Standard deviation (N/cm)	0.175	0.085	0.225	0.085	0.350	0.263

TABLE VI. Experimental peeling force data for 100 mesh forming belt

	Fabric processed with 50 g/m <sup>2</sup> web			Fabric processed with 100 g/m <sup>2</sup> web		
	9	14	20	9	14	20
Final jet pressure (MPa)	9	14	20	9	14	20
Peeling force (N/cm)	1.925	2.275	2.625	1.750	1.925	2.100
Standard deviation (N/cm)	0.105	0.175	0.070	0.085	0.035	0.158

(Figures 8a and 8b), where very few fibers are left caught in the knuckles. From the results given in Tables III through VI, it is evident that when the other process parameters are the same, the peeling force for a coarser mesh forming belt is larger than that for a finer mesh forming belt. Combining the information gained from the peeling force measurements and magnified photographs of the forming belt, it is concluded that the more fibers are caught in the knuckles of the forming belt, the larger is the peeling force required to separate the fabric from the forming belt.

Comparing the microscopic structures for different fiberwebs on the same forming belt, it is found that when the other processing conditions are the same, more fibers are caught by the forming wires for the fiberweb with a smaller basis weight after the fabric is separated. This is explained by the fact that it is easier for the water jets to penetrate through the lighter weight web, resulting in pushing more fibers into the knuckles of the forming belt. This phenomenon is obvious for the 10 mesh, 36 mesh and 75 mesh forming belts (see Figures 5 through 7). The effect of the fiberweb basis weight is not significant for the 100 mesh forming belt (see Figure 8). This is because so few fibers are caught by the 100 mesh forming wires regardless of the fiberweb basis weight. The corresponding peeling force results given in Tables III through VI also indicate that on any given type of the forming belt, the peeling force required to separate the fabric with a smaller basis weight is larger when the water jet pressure is the same.

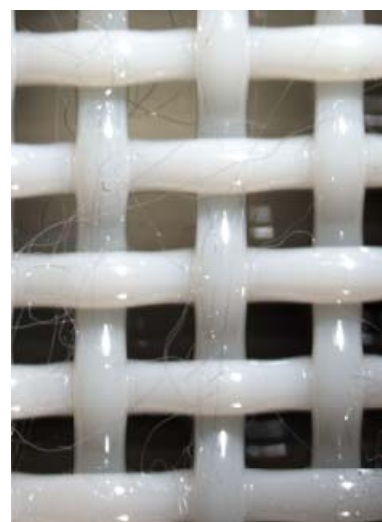
The peeling force results of Tables III through VI also support the conclusion that on any given type of a forming belt, the peeling force increases with the increase of the jet pressure for a given basis weight fiberweb.

From the above observations, it is concluded that the primary reason why a force is required to separate the

fabric from the forming belt is fiber entrapment in the knuckles of the forming wires.



(a) 50 g/m<sup>2</sup> web

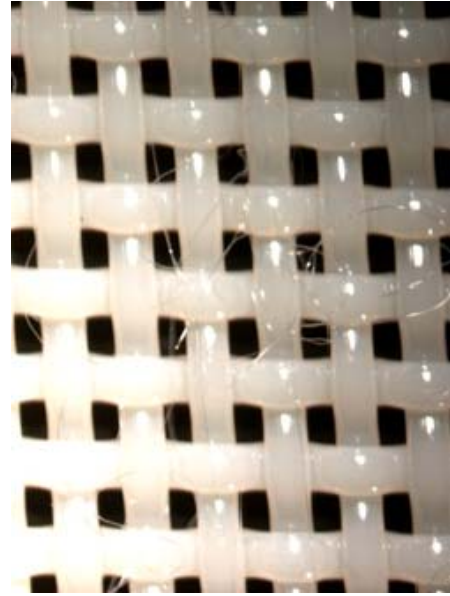


(b) 100 g/m<sup>2</sup> web

FIGURE 5. Magnified photographs of 10 mesh forming belts after fabric has been removed from them (final jet pressure: 200 bar, magnification: 0.8)

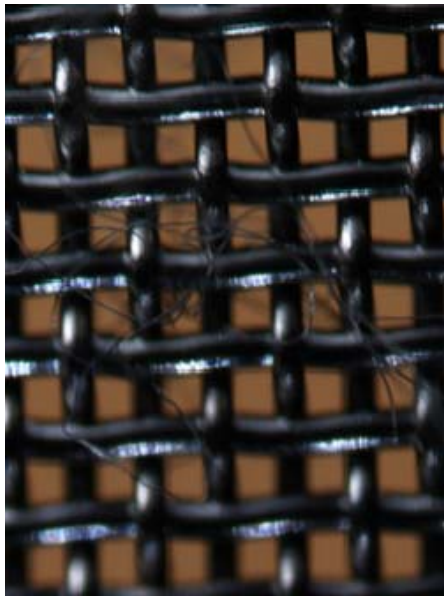


(a) 50 g/m<sup>2</sup> web

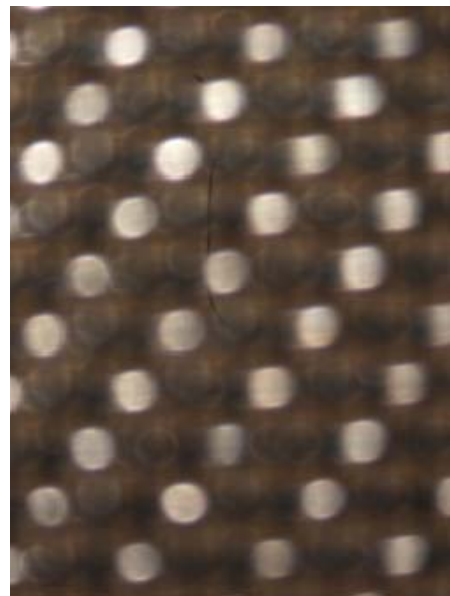


(b) 100 g/m<sup>2</sup> web

FIGURE 6. Magnified photographs of 36 mesh forming belts after fabric has been removed from them (final jet pressure: 200 bar, magnification: 1.5)



(a) 50 g/m<sup>2</sup> web



(b) 100 g/m<sup>2</sup> web

FIGURE 7. Magnified photographs of 75 mesh forming belts after fabric has been removed from them (final jet pressure: 200 bar, magnification: 3.0)



(a) 50 g/m<sup>2</sup> web



(b) 100 g/m<sup>2</sup> web

FIGURE 8. Magnified photographs of 100 mesh forming belts after fabric has been removed from them (final jet pressure: 200 bar, magnification: 5.0)

The physical reason why some fibers are caught in the knuckles of the forming wires is the entangling effect of the water jets, which, in addition to entangling fibers, also push some of the fibers into the spaces between the forming wires, rotate the fibers around the forming wires, and push the fibers into the knuckles. The mechanism of fiber entrapment in the knuckles can be described as follows. The impinging water induces vortices as it passes through the fiberweb and the voids between the forming wires. Due to the rotational effect of the water vortices, fibers swirl with water. By the combined effect of jet pressure and vorticity, some fibers are pushed directly into the knuckles, some other fibers and entangled around the forming wires in the MD-CD plane. The fibers entangled around the forming wires are then shifted and pushed into the knuckles by the water flow. As a result, most fibers entangled around the forming wires end up getting caught between the wires at knuckles; this leads to the force of peeling required for separating the fiberweb from the forming wires.

The fabric is strongly affected by the peeling process. Generally, for a larger peeling force, the regularity of the fabric is worse and there is higher probability to have damage on the fabric. For example, for the 50 g/m<sup>2</sup> web on the 10 mesh forming belt, the fabric is strongly distorted after the separation. However, for

the webs on the 100 mesh forming belt, the fabric exhibits only a very minor distortion after the separation from the forming belt. Typical fabric damage resulting from separating the fabric from the forming belt is shown in *Figure 2*.

#### **Prediction of the effect of separation speed**

The speed of separation of the fabric from the forming belt used in the experiments reported in this paper is 0.3 m/min, which is due to specifications of the Sintech tensile tester used in this research. This is significantly lower than a speed of separation used in industry for a typical hydroentanglement process (30 m/min). In this section an equation that predicts how to rescale the results obtained in the experiments for the case of a different separation speed is developed.

To better understand physical phenomena during the separation, the lengths of the fibers that are left caught in the knuckles after the separation are measured and the results are summarized in *Table VII*. The forming wires were cut and the fibers caught in the knuckles were carefully removed from the belts without breaking the fibers. With the aid of a ruler, the length of each fiber was measured. The fibers were manually straightened by removing the crimp without stretching. It is found that most fibers that are caught in the knuckles are broken during the separation process. This suggests that the dependence

of the peeling force on the separation velocity can be deduced from the relation between tenacity and rate of extension, which is given in [13] as:

$$F_1 - F_2 = kF_1 \log_{10}(t_2 / t_1) \quad (1)$$

where  $F_1$  is the breaking load if the fiber breaks over the time interval  $t_1$ ,  $F_2$  is the breaking load if the fiber breaks over the time interval  $t_2$ , and  $k$  is the strength-time coefficient. Values of the constant  $k$  are given in ref. [13] for different types of fibers. Thus, the peeling force  $F_p$  at a different separation speed can be estimated as:

$$F_{p1} - F_{p2} = kF_{p1} \log_{10}(t_2 / t_1) \quad (2)$$

Since  $v_1 \cdot t_1 = v_2 \cdot t_2$ , the above equation can be recast as:

$$F_{p2} = F_{p1} [1 - k \log_{10}(v_1 / v_2)] \quad (3)$$

where  $t_1$  is the separation time at the separation speed  $v_1$ ,  $F_{p1}$  is the peeling force at the separation speed  $v_1$ ,  $t_2$  is the separation time at the separation speed  $v_2$ , and  $F_{p2}$  is the peeling force measured at the separation speed  $v_2$ .

Therefore, using the measured peeling force at a separation speed of 0.3 m/min, the peeling force at any other separation speed can be predicted using Eq. (3). It is obvious from Eq. (3) that the peeling force increases when the separation speed is increased. While the results of Tables III-VI show the peeling forces measured at very low speed compared to the real process speed, the effects of the forming belt mesh size, jet pressure, and web basis weight on the peeling force will not change with the separation speed.

TABLE VII. Length of fibers that are left caught in the knuckles of the forming belt after separating the forming belt from the fabric

Forming belt	Mean fiber length	Standard deviation of fiber length	Number of fibers measured
10 mesh	18.1 mm	8.8 mm	26
36 mesh	15.5 mm	9.4 mm	26
75 mesh	10.2 mm	4.3 mm	15
100 mesh	6.0 mm	1.2 mm	8

## CONCLUSIONS

This paper details experimental investigation of the peeling force required for separating the hydroentangled fabric from the forming belt. The peeling force is measured for fiberwebs with different basis weights formed with different jet pressure on different forming belts. It is found that for any given type of a forming belt, the peeling force increases with the increase of the jet pressure for a given basis weight of the fiberweb, and increases with the decrease of the fiberweb basis weight at a given jet pressure. It is also found that when the other process parameters are the same, the use of a coarser mesh forming belt leads to more fibers caught between the wires in the knuckles, hence a larger peeling force.

The magnified images of the forming belt show that after the fabric is separated from the forming belt, some fibers are left caught by the wires. For a coarser mesh forming belt, more fibers are left caught by the forming wires for a given jet pressure and fiberweb. When other processing conditions are the same, more fibers are left caught by the wires for the fiberweb with a smaller basis weight after the fabric is removed. It is concluded that the primary reason why a force is required to separate the fabric from the forming belt is fiber entrapment (fibers are entangled around the wires and pushed into the knuckles) by the forming wires. These fibers are held tightly by the forming wires and the entangled fiberweb and break during to the fabric separation from the forming belt thus generating the peeling force.

## ACKNOWLEDGEMENT

The support provided by the Nonwoven Cooperative Research Center of North Carolina State University is gratefully acknowledged. Helpful discussions with industry advisors of this project, C. Camelio, R. Holmes, F. Noëlle, Dr. D. Shiffler and C. B. Widen, are greatly appreciated.

## REFERENCES

- [1] Tafreshi H. V., and Pourdeyhimi B., 2003. The effects of nozzle geometry on waterjet breakup at high reynolds numbers, *Experiments in Fluids* **35**, pp. 364–371
- [2] Anantharamaiah N., Tafreshi H. V., and Pourdeyhimi B., 2006. A study on hydroentangling waterjets and their impact forces, *Experiments in Fluids* **41** (1), pp. 103-113



- [3] Tafreshi H. V., and Pourdeyhimi B., 2004. Simulation of cavitation and hydraulic flip inside hydroentangling nozzles, *Textile Research Journal* **74** (4), pp. 359–364
- [4] Tafreshi H. V., and Pourdeyhimi B., 2004. Cavitation and hydraulic flip, *Fluent News* **13** (1), pp. 38
- [5] Pourmohammadi A., Russell S. J., Höffle S., 2003. Effect of water jet pressure profile and initial web geometry on the physical properties of composite hydroentangled fabrics. *Textile Research Journal*, 73, pp. 503-508
- [6] Ghassemieh E., Acar M., Versteeg H. K., 2001. Improvement of the efficiency of energy transfer in the hydro-entanglement process. *Composites Science and Technology*, 61, pp. 1681-1694
- [7] Ghassemieh E., Acar M., Versteeg H. K., Microstructural analysis of non-woven fabrics using scanning electron microscopy and image processing. Part 2: application to hydroentangled fabrics, 2002. *Proceedings of the Institution Mechanical Engineers, Part L, Journal of Materials: Design and Applications*, vol. 216, No. 4, pp. 211-218
- [8] Pourdeyhimi, B., Mintion A., Putnam, M., and Kim, H. S., 2004. Structure- Process-Property Relationships in Hydroentangled Nonwoven – Part 1: Preliminary Experimental Observations, *International Nonwoven Journal*, vol. 13, pp. 15-21
- [9] Villaume A. M., 1991. A global approach to the economics and end-product quality of spunlace non-wovens, *TAPPI Journal*, pp. 149-152
- [10] Berkalp, O. B., Pourdeyhimi, B., and Seyam, A., 2003. Texture Evolution in Hydroentangled Nonwovens, *International Nonwoven Journal*, vol. 12, pp. 28-35
- [11] Medeiros F. J., 1996. Spunlace/hydroentanglement methods and products. *INDATEC conference*, 5.1-5.15
- [12] Xiang P., Kuznetsov A.V., Seyam A.M., 2006. Experimental and numerical investigation of the peeling force required for the detachment of fabric from the forming belt in the hydroentanglement process, *Journal of Textile Institute*, Submitted
- [13] Morton W. E., and Hearle, J. W. S., 1975. Physical Properties of Textile Fibers, Halsted Press, New York, pp. 359-361

#### AUTHORS' ADDRESSES

##### **Abdelfattah Mohamed Seyam, Ph.D.**

College of Textiles  
North Carolina State University  
2401 Research Drive  
Raleigh, North Carolina 27695-8301  
USA

##### **Ping Xiang; Andrey V. Kuznetsov, Ph.D.**

Department of Mechanical and Aerospace  
Engineering  
College of Engineering  
Broughton Hall 3182  
North Carolina State University  
Raleigh, North Carolina 27695  
USA